

Cross second virial coefficients and dilute gas transport properties of the systems (CH₄ + C₂H₆) and (N₂ + C₂H₆) from accurate intermolecular potential energy surfaces

Robert Hellmann*

Institut für Chemie, Universität Rostock, 18059 Rostock, Germany

Abstract

The cross second virial coefficients and dilute gas shear viscosities, thermal conductivities, and binary diffusion coefficients of the systems (CH₄ + C₂H₆) and (N₂ + C₂H₆) were determined at temperatures from 90 K to 1200 K using statistical thermodynamics and the kinetic theory of molecular gases. The required intermolecular potential energy surfaces (PESs) for CH₄-C₂H₆ and N₂-C₂H₆ interactions are presented in this work, while the like-species interactions were modeled using PESs from our previous studies on the pure gases. All of these PESs are based on high-level quantum-chemical *ab initio* calculations and were fine-tuned to the most accurate experimental data available for the second virial and cross second virial coefficients. The agreement of the calculated values for all investigated thermophysical properties with the best experimental data is overall very satisfactory and confirms the high accuracy of the calculated values.

Keywords: methane, ethane, nitrogen, second virial coefficient, transport property

© 2019. This manuscript version is made available under the CC-BY-NC-ND 4.0 license.

<http://creativecommons.org/licenses/by-nc-nd/4.0/>

The published article is available at <https://doi.org/10.1016/j.jct.2019.03.002>.

1. Introduction

The calculation of the thermophysical properties of a fluid requires detailed knowledge of the potential energy surface (PES) governing the interactions between the molecules. In the limit of a dilute gas, the thermophysical properties are determined solely by binary interactions and thus by the pair potentials. Today, accurate representations of pair PESs can be constructed for interactions between simple molecules such as the natural gas components methane (CH₄) [1], ethane (C₂H₆) [2], propane (C₃H₈) [3], nitrogen (N₂) [4], carbon dioxide (CO₂) [5], and hydrogen sulfide (H₂S) [6] by fitting suitable analytical functions to interaction energies obtained from high-level quantum-chemical *ab initio* calculations. Once the pair potential functions are available, it is often straightforward to compute second virial and cross second virial coefficients employing standard expressions from statistical thermodynamics, while transport properties in the dilute gas limit are accessible through the kinetic theory of molecular gases [7–11].

In previous studies, we had investigated the cross second virial coefficients and dilute gas shear viscosities, thermal conductivities, and binary diffusion coefficients of several binary subsystems of natural gas involving the above-mentioned components, namely all six binary systems formed by CH₄, N₂, CO₂, and H₂S [9–13] as well as the mixtures (CH₄ + C₃H₈) [14] and (CO₂ + C₃H₈) [14]. These studies substantially improved our knowledge, since in many cases experimental data for the investigated thermophysical properties, if existing at all, are scarce, of low accuracy, or only available at or near ambient temperature.

The present study extends this investigation to the mixtures (CH₄ + C₂H₆) and (N₂ + C₂H₆) using the same proven methodologies. Since no analytical PESs of sufficient accuracy for CH₄-C₂H₆ and N₂-C₂H₆ interactions are available in the literature, we developed such PESs as part of this work and present them in the next section. The cross second virial coefficients and dilute gas shear viscosities, thermal conductivities, and binary diffusion coefficients were calculated for temperatures from 90 K to 1200 K. The respective methodologies are summarized in Section 3. The results are presented and discussed in Section 4, and practical correlations for the cross second virial and binary diffusion coefficients are provided in Section 5. Finally, conclusions are given in Section 6.

2. New potential energy surfaces for CH₄-C₂H₆ and N₂-C₂H₆ interactions

2.1. Calculation of interaction energies

The CH₄, N₂, and C₂H₆ molecules were treated as rigid rotors in all quantum-chemical *ab initio* calculations of CH₄-C₂H₆ and N₂-C₂H₆ interaction energies. The geometries

*Corresponding author

Email address: robert.hellmann@uni-rostock.de (Robert Hellmann)

were taken from our studies on the CH₄–CH₄ [1], N₂–N₂ [4], and C₂H₆–C₂H₆ [2] PESs and correspond to the zero-point vibrationally averaged structures. Each configuration of the molecule pairs can be expressed in terms of internal coordinates by the separation between the centers of mass of the two molecules, R , and five (for CH₄–C₂H₆) or four (for N₂–C₂H₆) angles, whose precise definition is provided in the [Supporting Information](#).

A total of 300 distinct CH₄–C₂H₆ angular orientations and 253 distinct N₂–C₂H₆ angular orientations was investigated. For each orientation, 27 center-of-mass separations R in the range from 1.5 Å to 12.0 Å were considered, resulting in 8100 (300 × 27) CH₄–C₂H₆ and 6831 (253 × 27) N₂–C₂H₆ configurations. However, many configurations with small R values were discarded because of excessive overlap of the molecules or because of problems in the quantum-chemical *ab initio* calculations related to near-linear dependencies in the basis sets, leaving 7134 CH₄–C₂H₆ and 6104 N₂–C₂H₆ configurations.

The interaction energy V for each configuration was obtained from counterpoise-corrected [15] supermolecular calculations. First, such calculations were carried out at the frozen-core resolution of identity second-order Møller–Plesset perturbation theory (RI-MP2) [16, 17] level with the RI-JK approximation [18, 19] for the Hartree–Fock (HF) part. The aug-cc-pVXZ [20, 21] basis sets with $X = 4$ (Q) and $X = 5$ were employed in these calculations. The auxiliary basis sets used for both basis set levels are aug-cc-pV5Z-JKFIT [22] and aug-cc-pV5Z-MP2FIT [23]. The correlation parts of the computed interaction energies, $V_{\text{RI-MP2 corr}}$, were extrapolated to the complete basis set (CBS) limit using the well-established two-point scheme recommended by Halkier et al. [24],

$$V_{\text{RI-MP2 corr}}(X) = V_{\text{RI-MP2 corr}}^{\text{CBS}} + \alpha X^{-3}. \quad (1)$$

The HF contributions are effectively converged at the $X = 5$ basis set level and were therefore not extrapolated. In the next step, counterpoise-corrected supermolecular calculations were also performed at the frozen-core coupled-cluster level with single, double, and perturbative triple excitations [CCSD(T)] [25] using the aug-cc-pVDZ and aug-cc-pVTZ basis sets for all configurations. Interaction energies at the MP2 level of theory were obtained as a byproduct of these calculations. The differences between the CCSD(T) and MP2 interaction energies were then extrapolated to the CBS limit in the same manner as $V_{\text{RI-MP2 corr}}$ and added to $V_{\text{RI-MP2}}^{\text{CBS}}$. In the well regions of the PESs, the interaction energies V thus obtained should correspond to within about $\pm(1-2)\%$ to the frozen-core CCSD(T)/CBS level.

The detailed results of the *ab initio* calculations for all investigated CH₄–C₂H₆ and N₂–C₂H₆ configurations are listed in the [Supporting Information](#). The RI-MP2 calculations were performed using ORCA 3.0.3 [26], while the CCSD(T) calculations were carried out using CFOUR [27].

2.2. Analytical potential functions

To obtain the CH₄–C₂H₆ and N₂–C₂H₆ PESs in analytical form, we fitted site–site potential functions with isotropic site–site interactions to the *ab initio* calculated interaction energies. As in our studies on the CH₄–CH₄ [1], N₂–N₂ [4], and

C₂H₆–C₂H₆ [2] PESs, the number of sites per molecule was chosen to be nine for CH₄, five for N₂, and eleven for C₂H₆. The positions of the sites within the molecules, which are visualized in Fig. 1, and their partial charges q were also taken from the earlier studies. Due to symmetry, there are three types of sites each in CH₄ and N₂ and four types in C₂H₆, resulting in 12 types of site–site interactions for each PES. The site–site interactions are represented by

$$V_{ij}(R_{ij}) = A_{ij} \exp(-\alpha_{ij} R_{ij}) - f_6(b_{ij}, R_{ij}) \frac{C_{6ij}}{R_{ij}^6} + \frac{q_i q_j}{R_{ij}}, \quad (2)$$

where R_{ij} is the separation between site i in CH₄ or N₂ and site j in C₂H₆, and f_6 is a damping function [28],

$$f_6(b_{ij}, R_{ij}) = 1 - \exp(-b_{ij} R_{ij}) \sum_{k=0}^6 \frac{(b_{ij} R_{ij})^k}{k!}. \quad (3)$$

The total interaction potentials are then obtained as the sums over all site–site interactions,

$$V = \sum_i \sum_j V_{ij}(R_{ij}). \quad (4)$$

The parameters A , α , b , and C_6 for the 12 distinct site–site combinations per PES were optimized in non-linear least-squares fits to the *ab initio* calculated interaction energies using weighting functions w given by

$$w = \frac{\exp\left[a_1 \left(\frac{R}{\text{Å}}\right)^3\right]}{\left[1 + a_2 (V/\text{K} + a_3)^2\right]^2}, \quad (5)$$

where $a_1 = 0.003$, $a_2 = 10^{-6}$, and $a_3 = 450$ for CH₄–C₂H₆ and $a_3 = 350$ for N₂–C₂H₆. The denominator of this function causes the weight of configurations to increase as the interaction energy decreases toward the most negative values ($V > -450$ K and $V > -350$ K for all investigated CH₄–C₂H₆ and N₂–C₂H₆ configurations, respectively), while the numerator ensures a high fit quality for large values of R , which is particularly important for the calculation of the cross second virial coefficients. Similar weighting functions were also used in several of our previous studies (e.g., in Ref. [12]). Note that in this work we quote energies always in units of kelvin, i.e., we divide them by Boltzmann’s constant k_B but omit k_B from the notation for brevity.

Figure 2 shows the deviations of the fitted interaction energies for both molecule pairs from the corresponding *ab initio* calculated ones as a function of the latter up to 8000 K (with the full range of investigated interaction energies extending up to almost 200,000 K for some angular orientations). It can be seen in the figure that the relative deviations are mostly within $\pm 2\%$, which is acceptable considering that the fitting errors with positive and negative sign can be expected to largely cancel out when calculating thermophysical properties. We note that the lowest unphysical maxima of the analytical potential functions (which are pure fitting artifacts) occur only at interaction energies of about 118,000 K for CH₄–C₂H₆ and about 83,000 K for

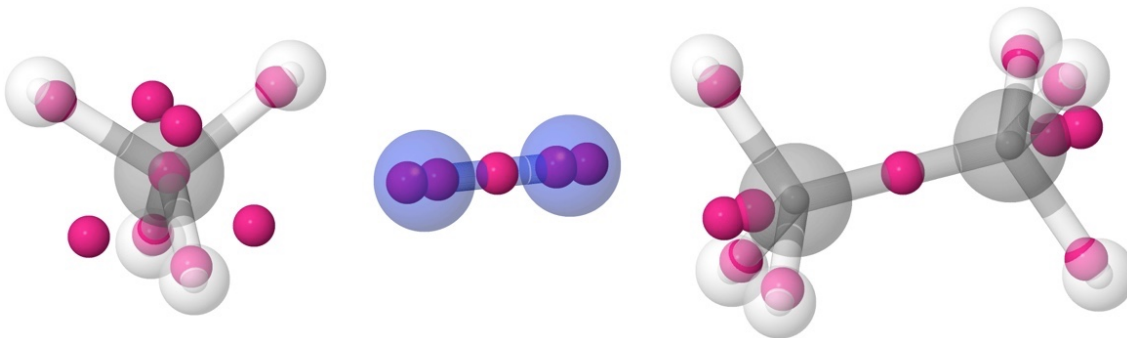


Figure 1: Visualization of the positions of the nine interaction sites in CH_4 used by the $\text{CH}_4\text{-CH}_4$ PES of Ref. [1], the five interaction sites in N_2 used by the $\text{N}_2\text{-N}_2$ PES of Ref. [4], and the eleven interaction sites in C_2H_6 used by the $\text{C}_2\text{H}_6\text{-C}_2\text{H}_6$ PES of Ref. [2]. These sites were also used for the new analytical $\text{CH}_4\text{-C}_2\text{H}_6$ and $\text{N}_2\text{-C}_2\text{H}_6$ potential functions of the present study.

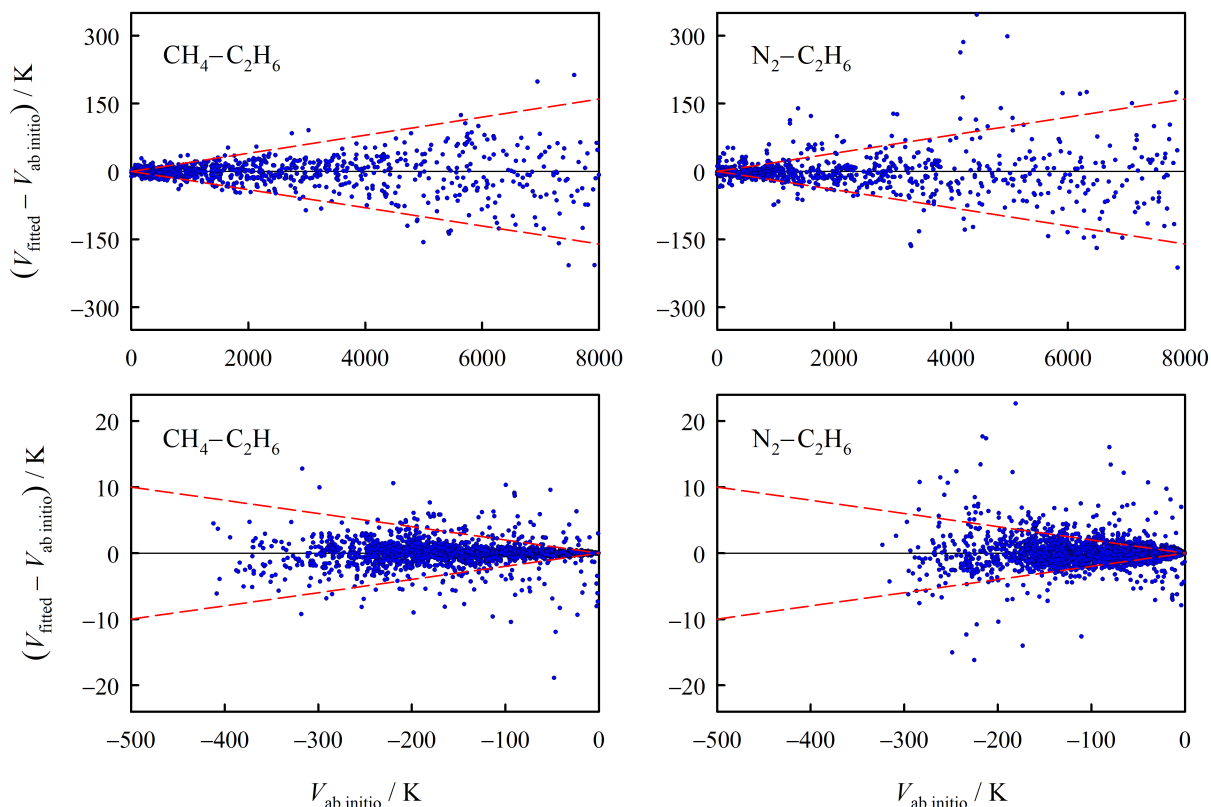


Figure 2: Deviations of interaction energies obtained using the fitted analytical potential functions for the $\text{CH}_4\text{-C}_2\text{H}_6$ and $\text{N}_2\text{-C}_2\text{H}_6$ molecule pairs from the corresponding *ab initio* calculated values as a function of the latter. The dashed lines indicate relative deviations of $\pm 2\%$.

$\text{N}_2\text{-C}_2\text{H}_6$. This is unproblematic for the thermophysical property calculations of this work.

Figures 3 and 4 illustrate the separation dependences of the new analytical potential functions in the well regions for a few selected angular orientations of the $\text{CH}_4\text{-C}_2\text{H}_6$ and $\text{N}_2\text{-C}_2\text{H}_6$ molecule pairs, respectively. The corresponding *ab initio* calculated interaction energies are also displayed in the figures. The analytical $\text{CH}_4\text{-C}_2\text{H}_6$ PES features three symmetry-distinct minima, with the interaction energy of the global minimum

being -430.4 K. The analytical $\text{N}_2\text{-C}_2\text{H}_6$ PES has only two symmetry-distinct minima, with the interaction energy of the global minimum being -351.2 K.

In our previous studies on *ab initio* intermolecular PESs that involve hydrocarbons [1–3, 9, 11, 14], we always found systematic positive deviations of the calculated values for the second virial and cross second virial coefficients from most of the available experimental data. This can be attributed mainly to the use of rigid monomers, which particularly for the hydrocarbons

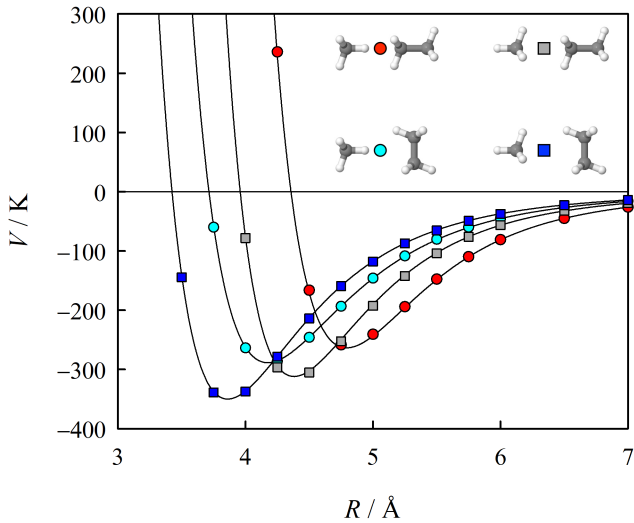


Figure 3: $\text{CH}_4\text{-C}_2\text{H}_6$ pair potential as a function of the center-of-mass separation R for four of the 300 considered angular orientations. The symbols represent the *ab initio* values and the solid lines the fitted potential function.

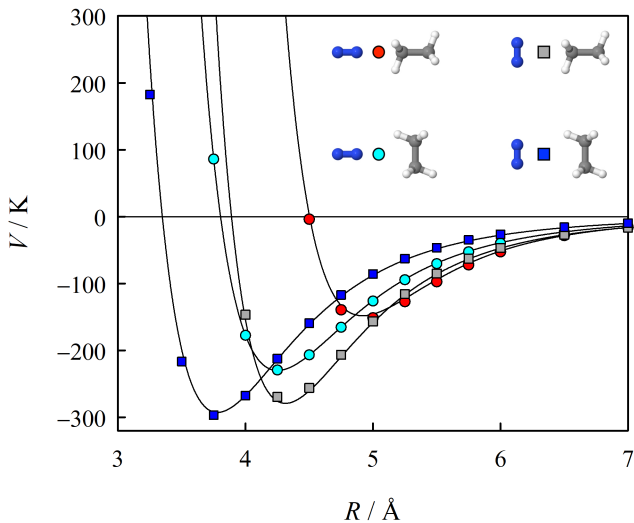


Figure 4: $\text{N}_2\text{-C}_2\text{H}_6$ pair potential as a function of the center-of-mass separation R for four of the 253 considered angular orientations. The symbols represent the *ab initio* values and the solid lines the fitted potential function.

results in the neglect of important vibrational contributions to the dispersion coefficients, see Ref. [29] and references therein. These contributions are only partly accounted for by the use of vibrationally averaged monomer geometries in the *ab initio* computations. However, for our previously developed PESs involving hydrocarbons [1–3, 9, 11, 14], a simple correction to the dispersion part with only one empirically adjusted parameter was always found to be sufficient to bring the calculated values and the best experimental data into satisfying agreement. In the present work, we adjusted the analytical $\text{CH}_4\text{-C}_2\text{H}_6$ PES

by changing the C_6 parameter for the interactions of the site on the carbon atom of CH_4 with the two sites closest to the two carbon atoms of C_2H_6 by an amount that was adjusted by trial and error to the best experimental data for the cross second virial coefficient (see Section 4.1). For the analytical $\text{N}_2\text{-C}_2\text{H}_6$ PES, the respective adjustment was performed by changing the C_6 parameter for the interactions of the two sites closest to the two nitrogen atoms with the two sites closest to the two carbon atoms. The adjustment procedure increases the maximum well depth of the $\text{CH}_4\text{-C}_2\text{H}_6$ PES from 430.4 K to 443.4 K and that of the $\text{N}_2\text{-C}_2\text{H}_6$ PES from 351.2 K to 352.4 K. That the required adjustment is much smaller for the $\text{N}_2\text{-C}_2\text{H}_6$ potential is somewhat expected because only one of the two molecules is a hydrocarbon. However, the very small magnitude of the adjustment indicates that other errors [such as the neglect of post-CCSD(T) contributions to the interaction energies] partly cancel the underestimation of the strength of the dispersion interactions due to the rigid-rotor approximation. Unless otherwise noted, all thermophysical property values reported in this work were obtained with the adjusted PESs.

Details of the symmetry-distinct minima for both the unadjusted and the adjusted analytical potential functions are given in the [Supporting Information](#), which also provides Fortran 90 routines that compute the new PESs.

3. Calculation of thermophysical properties

3.1. Cross second virial coefficients

For a pair of rigid molecules, the classical-mechanical cross second virial coefficient is given as

$$B_{12}^{\text{cl}} = -\frac{N_A}{2} \int_0^\infty \left\langle \exp \left[-\frac{V(\mathbf{R}, \Omega_1, \Omega_2)}{k_B T} \right] - 1 \right\rangle_{\Omega_1, \Omega_2} d\mathbf{R}, \quad (6)$$

where N_A is Avogadro's constant, T is the temperature, \mathbf{R} is the separation vector between the centers of mass of the two molecules, Ω_1 and Ω_2 represent their angular orientations, and the angle brackets indicate a proper averaging over the orientations. The masses and moments of inertia of CH_4 , N_2 , and C_2H_6 are large enough to justify accounting for quantum effects in a semiclassical manner at all temperatures of interest by replacing the pair potential V in Eq. (6) by the quadratic Feynman–Hibbs (QFH) effective pair potential [30]. For the $\text{CH}_4\text{-C}_2\text{H}_6$ pair, it can be written as

$$V_{\text{QFH}} = V + \frac{\hbar^2}{24k_B T} \left[\frac{1}{\mu} \left(\frac{\partial^2 V}{\partial x^2} + \frac{\partial^2 V}{\partial y^2} + \frac{\partial^2 V}{\partial z^2} \right) + \frac{1}{I_1} \left(\frac{\partial^2 V}{\partial \psi_{1a}^2} + \frac{\partial^2 V}{\partial \psi_{1b}^2} + \frac{\partial^2 V}{\partial \psi_{1c}^2} \right) + \frac{1}{I_{2\parallel}} \frac{\partial^2 V}{\partial \psi_{2a}^2} + \frac{1}{I_{2\perp}} \left(\frac{\partial^2 V}{\partial \psi_{2b}^2} + \frac{\partial^2 V}{\partial \psi_{2c}^2} \right) \right], \quad (7)$$

where \hbar is Planck's constant divided by 2π ; μ is the reduced mass of the two molecules; x , y , and z are the Cartesian components of \mathbf{R} ; I_1 denotes the moment of inertia of molecule 1 (CH_4); $I_{2\parallel}$ and $I_{2\perp}$ are the moments of inertia parallel and perpendicular to the figure axis of molecule 2 (C_2H_6); and the angles ψ_{1a} , ψ_{1b} , ψ_{1c} , ψ_{2a} , ψ_{2b} , and ψ_{2c} correspond to rotations around the principal axes of the molecules, with axis a

of molecule 2 being the figure axis. The expression for the QFH potential of the $\text{N}_2\text{-C}_2\text{H}_6$ molecule pair is of similar structure.

The cross second virial coefficients of the $\text{CH}_4\text{-C}_2\text{H}_6$ and $\text{N}_2\text{-C}_2\text{H}_6$ pairs were computed for 110 temperatures in the range from 90 K to 1200 K by means of the Mayer-sampling Monte Carlo (MSMC) approach of Singh and Kofke [31]. Hard spheres with a diameter of 4.5 Å were employed as the reference system. The results were obtained at all temperatures simultaneously by performing multi-temperature simulations [31, 32], in which the temperature governing the sampling distribution was chosen to be 120 K. To avoid unphysical negative interaction energies at very small intermolecular separations R , we placed hard spheres of 1.0 Å diameter on all interaction sites of the molecules. In each attempted MSMC move, one of the molecules was displaced and rotated. Maximum step sizes were adjusted during short equilibration runs to yield acceptance rates of 50%. The second derivatives of the pair potential needed to compute the QFH potential, see Eq. (7), were implemented analytically. For each molecule pair, values for the cross second virial coefficient from 16 independent simulation runs of 2×10^{10} attempted moves were averaged. The standard uncertainties of these averages due to the Monte Carlo integration do not exceed $0.015 \text{ cm}^3\cdot\text{mol}^{-1}$ at any temperature and are hence negligible.

3.2. Dilute gas transport properties

The kinetic theory of molecular gases [7–11, 33–38] is the most advanced approach available today for the calculation of transport properties of molecular gases and their mixtures in the zero-density limit with high accuracy and precision. For each transport property, a system of linear equations has to be solved, whose coefficients are given in terms of generalized cross sections. These cross sections are determined by the binary collisions between the molecules in the gas and are thus directly linked to the intermolecular potentials. In the present work, we calculated the shear viscosity η in the third-order kinetic theory approximation, the thermal conductivity λ (under steady-state conditions, see Ref. [10] for details) in the second-order kinetic theory approximation, and the product of molar density ρ_m and binary diffusion coefficient D in the third-order kinetic theory approximation from the generalized cross sections. The expressions for the respective systems of linear equations were already provided in previous papers [9–11] and are therefore not repeated here.

The approach for the computation of the thermal conductivity [10] requires the vibrational contributions to the ideal gas heat capacities of the gases, which we extracted from the recommended reference correlations for the isochoric ideal gas heat capacities [39–41] by subtracting the translational and classical rotational contributions.

The generalized cross sections for $\text{CH}_4\text{-C}_2\text{H}_6$ and $\text{N}_2\text{-C}_2\text{H}_6$ collisions were calculated within the rigid-rotor approximation by means of the classical trajectory method using an extended version of the TRAJECT code [8, 9, 38]. Collision trajectories were obtained by integrating Hamilton’s equations from pre- to post-collisional values. The initial and final separation was set

to 500 Å to avoid any PES cut-off effects. The integration accuracy was chosen such that the relative drift in the total energy between the initial and final states of the trajectories was usually in the range from 10^{-9} to 10^{-6} , with the maximum tolerated relative drift being 10^{-4} . Total-energy-dependent generalized cross sections in the center-of-mass frame, which can be formulated as multi-dimensional integrals over the initial states of the trajectories, were obtained from the initial and final states by means of a simple Monte Carlo integration scheme employing quasi-random numbers. The trajectory calculations were carried out for 37 values of the total energy, $E_{\text{total}} = E_{\text{trans}} + E_{\text{rot}}$, which was divided into the ranges $30 \leq E_{\text{total}}/\text{K} \leq 200$, $200 \leq E_{\text{total}}/\text{K} \leq 2000$, and $2000 \leq E_{\text{total}}/\text{K} \leq 30,000$. The 13 energies in each of the three ranges were chosen as the nodes for Chebyshev interpolation of the cross sections as a function of $\ln(E_{\text{total}})$. Up to 4×10^6 collision trajectories were generated at each value of the total energy. Below $E_{\text{total}} = 200 \text{ K}$, the number of trajectories had to be gradually reduced down to 400,000 at $E_{\text{total}} = 30 \text{ K}$ because of the high computational costs associated with the accurate calculation of trajectories at very low energies. A weighted integration over the total energy (thermal averaging) yielded temperature-dependent generalized cross sections in the center-of-mass frame at temperatures from 90 K to 1200 K, which were then converted to the laboratory frame cross sections needed in the systems of linear equations which have to be solved to obtain the three transport properties.

The required generalized cross sections for $\text{CH}_4\text{-CH}_4$, $\text{N}_2\text{-N}_2$, and $\text{C}_2\text{H}_6\text{-C}_2\text{H}_6$ collisions were determined from state-of-the-art pair potentials [1, 2, 4] in previous studies [2, 9] in a similar way as described here for $\text{CH}_4\text{-C}_2\text{H}_6$ and $\text{N}_2\text{-C}_2\text{H}_6$ collisions.

The relative standard uncertainties of the calculated transport property values for all temperatures and mole fractions due to the above-mentioned Monte Carlo integration scheme are estimated (based on uncertainty estimates generated by TRAJECT for the individual cross sections as described in Ref. [42]) to be less than 0.1% for the viscosity and the binary diffusion coefficient and less than 0.2% for the thermal conductivity. Any errors resulting from the numerical integration of Hamilton’s equations and from the Chebyshev interpolation of the total-energy-dependent generalized cross sections and the subsequent thermal averaging should be completely negligible.

4. Results and discussion

4.1. Cross second virial coefficients

Table 1 lists the semiclassically calculated values for the cross second virial coefficients of both molecule pairs, B_{12}^{QFH} , at 37 selected temperatures and our estimates of their combined expanded uncertainties (coverage factor $k = 2$, corresponding approximately to a 95% confidence level), $U(B_{12}^{\text{QFH}})$, which are discussed below.

Figure 5 shows the comparison of the calculated values for the cross second virial coefficient of the $\text{CH}_4\text{-C}_2\text{H}_6$ molecule pair with most of the available experimental data [43–50] and with the experimentally based correlation by Dymond

Table 1: Semiclassically calculated values for the cross second virial coefficients, B_{12}^{QFH} , of the $\text{CH}_4\text{-C}_2\text{H}_6$ and $\text{N}_2\text{-C}_2\text{H}_6$ molecule pairs and their estimated combined expanded uncertainties ($k = 2$), $U(B_{12}^{\text{QFH}})$, as a function of temperature T . The corresponding values for the second virial coefficients of the pure gases can be found in Refs. [1], [2], and [4].

T	$\text{CH}_4\text{-C}_2\text{H}_6$		$\text{N}_2\text{-C}_2\text{H}_6$	
	B_{12}^{QFH}	$U(B_{12}^{\text{QFH}})$	B_{12}^{QFH}	$U(B_{12}^{\text{QFH}})$
K	$\text{cm}^3\cdot\text{mol}^{-1}$	$\text{cm}^3\cdot\text{mol}^{-1}$	$\text{cm}^3\cdot\text{mol}^{-1}$	$\text{cm}^3\cdot\text{mol}^{-1}$
90	-1150	27	-606.3	15.7
100	-880.2	18.6	-480.9	11.6
110	-702.5	13.6	-393.6	9.1
120	-578.1	10.5	-329.5	7.3
130	-486.7	8.4	-280.7	6.1
140	-417.1	6.9	-242.4	5.2
150	-362.5	5.8	-211.5	4.5
160	-318.7	5.0	-186.1	4.0
170	-282.7	4.4	-164.9	3.6
180	-252.7	3.9	-147.0	3.2
190	-227.3	3.5	-131.6	2.9
200	-205.6	3.2	-118.3	2.7
220	-170.4	2.7	-96.30	2.3
240	-143.2	2.3	-79.01	2.0
260	-121.4	2.0	-65.05	1.8
280	-103.8	1.8	-53.56	1.6
300	-89.11	1.6	-43.95	1.5
320	-76.78	1.4	-35.79	1.4
340	-66.25	1.3	-28.80	1.3
360	-57.18	1.2	-22.73	1.2
380	-49.28	1.1	-17.43	1.1
400	-42.34	1.1	-12.76	1.0
420	-36.20	1.0	-8.62	1.0
440	-30.74	1.0	-4.92	1.0
460	-25.85	1.0	-1.60	1.0
480	-21.45	1.0	1.39	1.0
500	-17.46	1.0	4.10	1.0
550	-9.00	1.0	9.86	1.0
600	-2.19	1.0	14.50	1.0
650	3.39	1.0	18.31	1.0
700	8.04	1.0	21.47	1.0
750	11.96	1.0	24.13	1.0
800	15.30	1.0	26.40	1.0
900	20.69	1.0	30.02	1.0
1000	24.80	1.0	32.77	1.0
1100	28.03	1.0	34.89	1.0
1200	30.60	1.0	36.57	1.0

et al. [51]. We reanalyzed the data of Dantzler et al. [43] using our own values for the pure-component virial coefficients [1, 2], which are more accurate than the values used by Dantzler et al. Note that the error bars shown in Fig. 5 (and all following figures in which calculated thermophysical property values are compared with experimental data) correspond to those given by the respective authors. Only in the case of the reanalyzed data of Dantzler et al., we also reassessed the uncertainties. For the empirical adjustment of the analytical potential function described in Section 2.2, we used particularly the data close to room temperature of Jaeschke et al. [46], Trusler et al. [48], Blanke and Weiss [49], and Hou et al. [50] as reference. The adjustment changes the cross second virial coefficient by $-97.5 \text{ cm}^3\cdot\text{mol}^{-1}$ at $T = 90 \text{ K}$, $-7.3 \text{ cm}^3\cdot\text{mol}^{-1}$ at $T = 300 \text{ K}$, and $-1.5 \text{ cm}^3\cdot\text{mol}^{-1}$ at $T = 1200 \text{ K}$ and, as can be seen in the figure, results in a substantially improved

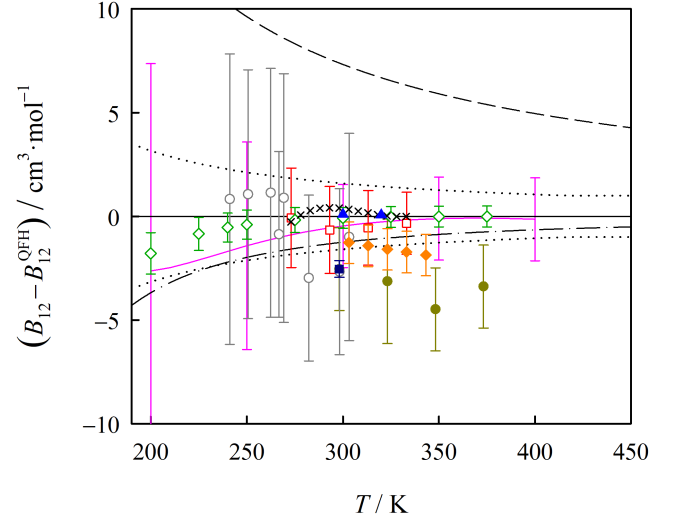


Figure 5: Deviations of experimental data, an experimentally based correlation, and calculated values for the cross second virial coefficient of the $\text{CH}_4\text{-C}_2\text{H}_6$ molecule pair from the semiclassically calculated values of the present work as a function of temperature: \bullet , Dantzler et al. [43], reanalyzed; \circ , Wormald et al. [44]; \blacksquare , Katayama et al. [45]; \square , Jaeschke et al. [46]; \blacklozenge , McElroy and Fang [47]; \diamond , Trusler [48]; \times , Blanke and Weiss [49] (provided by the authors only in the form of a smoothing function); \blacktriangle , Hou et al. [50]; solid line, correlation by Dymond et al. [51]; dashed line, semiclassical result for the unadjusted $\text{CH}_4\text{-C}_2\text{H}_6$ PES; dash-dot line, classical result for the adjusted $\text{CH}_4\text{-C}_2\text{H}_6$ PES; dotted lines, $B_{12}^{\text{QFH}} \pm U(B_{12}^{\text{QFH}})$ with $k = 2$.

agreement with the experimental data and the correlation of Dymond et al. The figure also depicts the classically calculated values obtained using the adjusted PES, which differ from the corresponding semiclassical values by $-76.8 \text{ cm}^3\cdot\text{mol}^{-1}$ at $T = 90 \text{ K}$, $-1.2 \text{ cm}^3\cdot\text{mol}^{-1}$ at $T = 300 \text{ K}$, and $-0.09 \text{ cm}^3\cdot\text{mol}^{-1}$ at $T = 1200 \text{ K}$.

In Fig. 6, the calculated values for the cross second virial coefficient of the $\text{N}_2\text{-C}_2\text{H}_6$ molecule pair are compared with the experimental data of Achtermann et al. [52] and Lopatinskii et al. [53], which are the only available high-quality data. The figure shows that only a very small adjustment of the analytical PES is needed (as already mentioned in Section 2.2) to bring the calculated values into agreement with all experimental data points within their uncertainties. The adjustment changes the cross second virial coefficient by $-4.5 \text{ cm}^3\cdot\text{mol}^{-1}$ at $T = 90 \text{ K}$, $-0.47 \text{ cm}^3\cdot\text{mol}^{-1}$ at $T = 300 \text{ K}$, and $-0.11 \text{ cm}^3\cdot\text{mol}^{-1}$ at $T = 1200 \text{ K}$. The classical values obtained with the adjusted PES are also shown in the figure. They differ from the corresponding semiclassically calculated values by $-21.7 \text{ cm}^3\cdot\text{mol}^{-1}$ at $T = 90 \text{ K}$, $-0.59 \text{ cm}^3\cdot\text{mol}^{-1}$ at $T = 300 \text{ K}$, and $-0.05 \text{ cm}^3\cdot\text{mol}^{-1}$ at $T = 1200 \text{ K}$.

Our estimates for the combined expanded uncertainties ($k = 2$) of the calculated values for the cross second virial coefficients of the two molecule pairs, which are based predominantly on the comparisons with the experimental data, are given

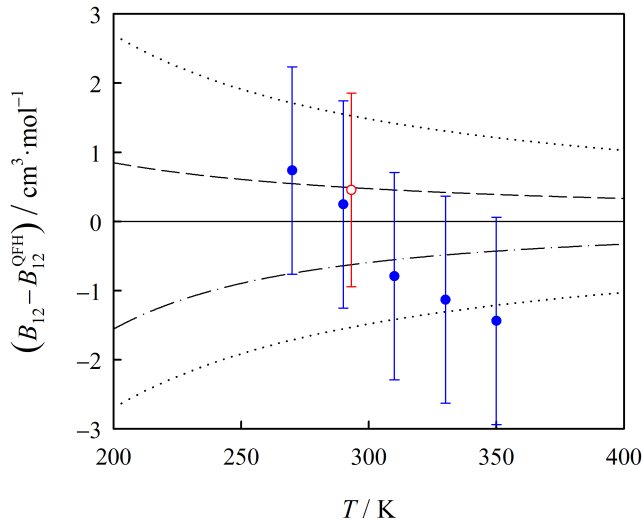


Figure 6: Deviations of experimental data and calculated values for the cross second virial coefficient of the $\text{N}_2\text{-C}_2\text{H}_6$ molecule pair from the semiclassically calculated values of the present work as a function of temperature: \bullet , Achtermann et al. [52]; \circ , Lopatinskii et al. [53]; dashed line, semiclassical result for the unadjusted $\text{N}_2\text{-C}_2\text{H}_6$ PES; dash-dot line, classical result for the adjusted $\text{N}_2\text{-C}_2\text{H}_6$ PES; dotted lines, $B_{12}^{\text{QFH}} \pm U(B_{12}^{\text{QFH}})$ with $k = 2$.

as

$$U(B_{12}^{\text{QFH}}) = \max\left(a_1 |B_{12}^{\text{QFH}} - B_{12,\text{unadj}}^{\text{QFH}}| + a_2 |B_{12}^{\text{QFH}} - B_{12}^{\text{cl}}|, a_3\right), \quad (8)$$

where $B_{12,\text{unadj}}^{\text{QFH}}$ are the semiclassical values obtained with the unadjusted PESs, $a_1 = 0.2$ for $\text{CH}_4\text{-C}_2\text{H}_6$ and $a_1 = 3.0$ for $\text{N}_2\text{-C}_2\text{H}_6$, $a_2 = 0.1$ (accounting for the fact that the semiclassical QFH approach is not exact), and $a_3 = 1.0 \text{ cm}^3 \cdot \text{mol}^{-1}$. The resulting uncertainty values are also depicted in Figs. 5 and 6. Note that real CH_4 and C_2H_6 molecules are unstable at the highest considered temperatures, but this is not taken into account in our uncertainty estimates for any of the thermophysical properties investigated in this work.

4.2. Dilute gas transport properties

The calculated values for the dilute gas shear viscosity η and thermal conductivity λ of both systems are listed for 26 temperatures and four mixture compositions in Tables 2 and 3. The viscosity and thermal conductivity values for the pure components, which were obtained in previous studies [2, 9, 10], are also listed there. The calculated values for the dilute gas limit of the product of molar density ρ_m and binary diffusion coefficient D are provided for the same 26 temperatures and for three mixture compositions in Table 4.

Figures 7 and 8 show the comparison of the calculated viscosity values with the data of Abe et al. [54, 55] for the two systems (which are the only available data sets for the mixtures) and with the data of Vogel [56, 57] and Vogel et al. [58] for the three pure gases. The data sets from the Vogel group extend from room temperature up to more than 600 K and

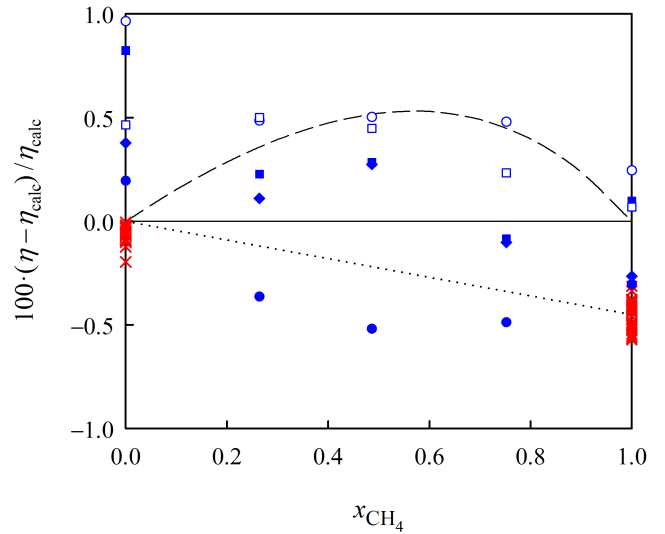


Figure 7: Relative deviations of experimental data for the dilute gas shear viscosity of the $(\text{CH}_4 + \text{C}_2\text{H}_6)$ system from the calculated values of the present work as a function of methane mole fraction: \bullet , Abe et al. [54], 298 K; \circ , Abe et al. [54], 333 K; \blacksquare , Abe et al. [54], 373 K; \square , Abe et al. [54], 418 K; \blacklozenge , Abe et al. [54], 468 K; \times , Vogel [56] and Vogel et al. [58], (290–682) K for methane and (291–624) K for ethane. The dashed and dotted lines indicate the values obtained with the unadjusted $\text{CH}_4\text{-C}_2\text{H}_6$ PES at $T = 300$ K and the recommended values resulting from Eq. 9, respectively. For clarity of the figure, the stated uncertainties for the data of Abe et al. [54] (0.3%), Vogel [56] (0.2%) and Vogel et al. [58] (0.3%) are not indicated by error bars.

are of reference quality with uncertainties of at most 0.3%. The relative deviations of these data from the calculated values are very weakly dependent on temperature and are on average only -0.45% for methane, $+0.24\%$ for nitrogen, and -0.07% for ethane, whereas the relative deviations of the data of Abe et al. [54, 55], for which the claimed uncertainty is also only 0.3%, are much more temperature dependent for both the pure components and the mixtures. The reason for this behavior is a design flaw in the viscometer employed by Abe et al., see the discussion in Ref. [59]. This resulted in viscosity values that are systematically too high above room temperature, with many recent studies [4, 9, 11, 12, 14, 56, 60] indicating that the overestimation can be up to about 1%, which is consistent with the behavior seen in Figs. 7 and 8.

As in our previous studies on the shear viscosities of binary gas mixtures [9, 11–14, 61], we propose a scaling of the calculated values by a temperature-independent factor that depends linearly on the mole fraction to obtain values with the lowest possible uncertainty:

$$\eta_{\text{rec}} = \eta_{\text{calc}} (0.9955x_{\text{CH}_4} + x_{\text{C}_2\text{H}_6}) \quad (9)$$

and

$$\eta_{\text{rec}} = \eta_{\text{calc}} (1.0024x_{\text{N}_2} + x_{\text{C}_2\text{H}_6}), \quad (10)$$

where η_{rec} and η_{calc} are the recommended and calculated viscosity values, respectively. The scaling factors 0.9955 for pure methane and 1.0024 for pure nitrogen remedy the small systematic deviations from the data of Vogel [56, 57] and were already

Table 2: Calculated values for the dilute gas shear viscosities η (in $\mu\text{Pa}\cdot\text{s}$) of the mixtures ($\text{CH}_4 + \text{C}_2\text{H}_6$) and ($\text{N}_2 + \text{C}_2\text{H}_6$) as a function of mole fraction x and temperature T . The values for the pure components, which were obtained in previous studies [2, 9], are also provided here.^a

T/K	CH_4	N_2	C_2H_6	CH_4 (1) + C_2H_6 (2)				N_2 (1) + C_2H_6 (2)			
				$x_1 = 0.2$	$x_1 = 0.4$	$x_1 = 0.6$	$x_1 = 0.8$	$x_1 = 0.2$	$x_1 = 0.4$	$x_1 = 0.6$	$x_1 = 0.8$
90	3.522	6.058	3.050	3.119	3.198	3.290	3.396	3.458	3.937	4.508	5.201
105	4.087	7.048	3.462	3.553	3.657	3.778	3.920	3.954	4.531	5.214	6.037
120	4.662	8.024	3.879	3.994	4.125	4.277	4.453	4.458	5.131	5.925	6.872
135	5.241	8.977	4.305	4.444	4.602	4.783	4.994	4.968	5.736	6.635	7.698
150	5.820	9.905	4.739	4.901	5.086	5.296	5.538	5.485	6.343	7.340	8.512
175	6.778	11.39	5.480	5.679	5.903	6.157	6.446	6.354	7.352	8.500	9.832
200	7.715	12.80	6.237	6.469	6.727	7.017	7.344	7.227	8.350	9.631	11.10
225	8.627	14.14	7.003	7.262	7.549	7.869	8.227	8.097	9.330	10.73	12.32
250	9.511	15.41	7.770	8.052	8.363	8.707	9.089	8.957	10.29	11.79	13.49
275	10.37	16.63	8.533	8.834	9.165	9.528	9.928	9.803	11.22	12.82	14.61
300	11.19	17.80	9.288	9.605	9.951	10.33	10.74	10.63	12.13	13.81	15.69
325	11.99	18.93	10.03	10.36	10.72	11.11	11.54	11.44	13.02	14.77	16.73
350	12.77	20.01	10.76	11.10	11.47	11.87	12.31	12.24	13.87	15.70	17.73
375	13.52	21.06	11.48	11.83	12.21	12.62	13.05	13.01	14.71	16.60	18.71
400	14.25	22.08	12.18	12.54	12.92	13.34	13.78	13.77	15.52	17.47	19.65
450	15.65	24.02	13.54	13.91	14.30	14.73	15.18	15.22	17.08	19.15	21.45
500	16.98	25.88	14.84	15.22	15.62	16.05	16.51	16.61	18.57	20.74	23.17
550	18.25	27.65	16.08	16.47	16.88	17.31	17.77	17.93	19.98	22.26	24.80
600	19.47	29.36	17.27	17.66	18.08	18.52	18.99	19.20	21.34	23.72	26.37
650	20.64	31.00	18.41	18.81	19.24	19.69	20.16	20.42	22.64	25.12	27.89
700	21.78	32.60	19.51	19.92	20.35	20.81	21.28	21.59	23.90	26.47	29.35
800	23.94	35.66	21.60	22.02	22.47	22.94	23.43	23.82	26.29	29.05	32.15
900	25.99	38.58	23.56	24.00	24.46	24.95	25.46	25.92	28.55	31.49	34.81
1000	27.94	41.38	25.42	25.87	26.35	26.86	27.39	27.91	30.70	33.82	37.36
1100	29.82	44.08	27.19	27.66	28.16	28.69	29.25	29.81	32.75	36.06	39.80
1200	31.64	46.70	28.88	29.37	29.90	30.45	31.03	31.64	34.73	38.21	42.17

^a The listed viscosity values should be scaled using Eqs. (9) and (10) to obtain the recommended values. The relative combined expanded uncertainty ($k = 2$) of the scaled values for the mixtures is estimated to be 1.0% for temperatures from 250 K to 700 K and 1.5% otherwise. The respective estimate for the scaled values of pure CH_4 is 0.4% from 300 K to 700 K, 0.8% from 200 K to 300 K and from 700 K to 1000 K, and 1.2% otherwise, that for the scaled values of pure N_2 is 0.3% from 300 K to 700 K and 1.0% otherwise, and that for the values of pure C_2H_6 is 0.3% from 250 K to 700 K and 1.0% otherwise.

recommended in our study on the ($\text{CH}_4 + \text{N}_2$) system [9]. For pure ethane [2], we did not recommend a scaling because of the almost perfect agreement with the data of Vogel et al. [58].

Figures 7 and 8 also show the results obtained with the unadjusted CH_4 - C_2H_6 and N_2 - C_2H_6 PESs at $T = 300$ K, where they differ from those obtained with the adjusted PESs by at most +0.53% for the ($\text{CH}_4 + \text{C}_2\text{H}_6$) system and +0.04% for the ($\text{N}_2 + \text{C}_2\text{H}_6$) system.

In Fig. 9, the calculated thermal conductivity values for the ($\text{CH}_4 + \text{C}_2\text{H}_6$) system are compared with the two available experimental data sets [62, 63] for the mixture and with the correlation by Friend and Roder [64] at four selected temperatures. The data of Roder and Friend [62] for the temperature range (194–330) K agree within $\pm 1.3\%$ with the calculated values above $T = 270$ K, which is consistent with the stated uncertainty for these data of 1.6%. However, the deviations become increasingly negative toward lower temperatures, with the largest deviation of -6.9% occurring at $T = 194$ K for a methane-rich mixture. The single datum of Sakonidou et al. [63] at $T = 311$ K for an equimolar mixture, for which no uncertainty estimate was provided, differs from the respective calculated value by +1.7%. The correlation by Friend and Roder [64] for temperatures from 140 K to 330 K, which is based on the data of Roder and Friend [62] and on data for the pure gases, exhibits negative deviations from the calculated val-

ues, which reach -13.6% at $T = 140$ K for pure ethane. However, one has to take into account that no experimental thermal conductivity data are available for ethane below $T = 225$ K [2] and that the functional form of the correlation in the zero-density limit is purely empirical and therefore not well suited for extrapolation from $T = 225$ K to temperatures as low as $T = 140$ K. Hence, the very large deviations at the lowest temperatures for ethane and ethane-rich mixtures are not meaningful.

The only available data set for the thermal conductivity of ($\text{N}_2 + \text{C}_2\text{H}_6$) mixtures is that of Gilmore and Comings [65] at a single temperature of 348 K. The stated uncertainty of these data is 3% and, as shown in Fig. 10, the agreement with the calculated values is within the experimental uncertainty.

In Figs. 9 and 10, we also show the results for the unadjusted CH_4 - C_2H_6 and N_2 - C_2H_6 PESs at $T = 300$ K. The relative deviations from the values for the adjusted PESs are close to those obtained in the case of the shear viscosity.

For the binary diffusion coefficient in the dilute gas phase, we found three experimental data sets for the ($\text{CH}_4 + \text{C}_2\text{H}_6$) system [66–68] and six such data sets for the ($\text{N}_2 + \text{C}_2\text{H}_6$) system [69–74]. They are compared with the calculated values in Figs. 11 and 12. The latter figure also depicts the correlation by Chae et al. [75] for the ($\text{N}_2 + \text{C}_2\text{H}_6$) system and temperatures from 500 K to 1000 K, which was fitted to diffusion

Table 3: Calculated values for the dilute gas thermal conductivities λ (in $\text{mW}\cdot\text{m}^{-1}\cdot\text{K}^{-1}$) of the mixtures ($\text{CH}_4 + \text{C}_2\text{H}_6$) and ($\text{N}_2 + \text{C}_2\text{H}_6$) as a function of mole fraction x and temperature T . The values for the pure components, which were obtained in previous studies [2, 10], are also provided here.^a

T/K	CH_4	N_2	C_2H_6	CH_4 (1) + C_2H_6 (2)				N_2 (1) + C_2H_6 (2)			
				$x_1 = 0.2$	$x_1 = 0.4$	$x_1 = 0.6$	$x_1 = 0.8$	$x_1 = 0.2$	$x_1 = 0.4$	$x_1 = 0.6$	$x_1 = 0.8$
90	9.343	8.255	4.357	5.054	5.866	6.822	7.962	4.864	5.468	6.200	7.106
105	10.97	9.699	5.100	5.916	6.867	7.990	9.335	5.705	6.423	7.290	8.356
120	12.64	11.13	5.893	6.828	7.918	9.208	10.75	6.594	7.422	8.415	9.626
135	14.33	12.55	6.742	7.792	9.019	10.47	12.21	7.531	8.460	9.566	10.90
150	16.04	13.93	7.652	8.813	10.17	11.77	13.69	8.521	9.538	10.74	12.18
175	18.89	16.16	9.326	10.66	12.21	14.04	16.22	10.30	11.43	12.75	14.31
200	21.77	18.29	11.23	12.70	14.42	16.44	18.84	12.26	13.45	14.83	16.43
225	24.70	20.33	13.39	14.98	16.83	19.00	21.58	14.43	15.62	16.98	18.55
250	27.75	22.28	15.82	17.51	19.47	21.76	24.48	16.81	17.94	19.22	20.66
275	30.96	24.15	18.53	20.31	22.36	24.75	27.57	19.42	20.42	21.54	22.79
300	34.37	25.94	21.51	23.36	25.49	27.97	30.88	22.24	23.05	23.95	24.92
325	37.98	27.68	24.74	26.66	28.86	31.42	34.42	25.26	25.83	26.44	27.07
350	41.81	29.37	28.20	30.19	32.46	35.09	38.17	28.46	28.73	29.00	29.23
375	45.84	31.02	31.87	33.92	36.26	38.97	42.12	31.82	31.75	31.62	31.40
400	50.06	32.63	35.71	37.83	40.25	43.03	46.26	35.32	34.87	34.31	33.59
450	59.01	35.80	43.81	46.08	48.66	51.61	55.02	42.66	41.34	39.81	38.00
500	68.52	38.92	52.32	54.77	57.53	60.68	64.30	50.31	48.04	45.45	42.45
550	78.46	42.02	61.11	63.75	66.72	70.11	73.98	58.18	54.90	51.19	46.94
600	88.76	45.11	70.08	72.94	76.15	79.80	83.96	66.20	61.86	56.99	51.46
650	99.33	48.20	79.16	82.26	85.75	89.68	94.17	74.30	68.89	62.83	55.99
700	110.1	51.29	88.31	91.68	95.45	99.71	104.6	82.45	75.95	68.69	60.53
800	132.1	57.44	106.7	110.6	115.0	120.0	125.7	98.78	90.08	80.41	69.60
900	154.5	63.51	124.9	129.5	134.7	140.5	147.0	115.0	104.1	92.02	78.57
1000	177.0	69.47	142.8	148.2	154.1	160.8	168.4	131.0	117.9	103.4	87.39
1100	199.3	75.30	160.4	166.5	173.2	180.9	189.5	146.6	131.4	114.6	96.01
1200	221.4	80.97	177.4	184.3	192.0	200.6	210.3	161.7	144.5	125.5	104.4

^a The relative combined expanded uncertainty ($k = 2$) of the values for the mixtures and for pure C_2H_6 is estimated to be 2.0% for temperatures from 250 K to 700 K and 3.0% otherwise. The respective estimate for the values of pure CH_4 is 1.0% from 300 K to 700 K, 1.5% from 200 K to 300 K and from 700 K to 1000 K, and 2.0% otherwise, and that for the values of pure N_2 is 1.0% from 300 K to 700 K and 2.0% otherwise.

coefficients obtained from molecular dynamics (MD) simulations. The two figures display the deviations from the calculated values as a function of temperature because the variation of $\rho_m D$ with mole fraction is very small; it does not exceed 0.81% for the ($\text{CH}_4 + \text{C}_2\text{H}_6$) system and 0.36% for the ($\text{N}_2 + \text{C}_2\text{H}_6$) system at any temperature. This is not surprising, since the mole fraction dependence of $\rho_m D$ is a higher-order kinetic theory effect. In the first-order approximation, $\rho_m D$ is mole fraction independent and, similarly to the cross second virial coefficient, determined entirely by the PES for the unlike-species interaction. This makes the binary diffusion coefficient the transport property that is most suited to validate unlike-species pair PESs provided that highly accurate experimental data are available. Unfortunately, as can be seen in the figures, the scatter of the experimental data is significant. However, for the ($\text{CH}_4 + \text{C}_2\text{H}_6$) system, the data of Arora et al. [68] (group of P. J. Dunlop) for temperatures from 275 K to 323 K differ from our calculated values only by about -0.5% . Diffusion coefficients measured by the Dunlop group are consistently in excellent agreement with the values obtained from accurate pair potentials in conjunction with the kinetic theory of gases as shown previously for the systems ($\text{Kr} + \text{He}$) [76] (within 0.3%), ($\text{CH}_4 + \text{C}_3\text{H}_8$) [14] (within 0.3%), and ($\text{CO}_2 + \text{N}_2$) [12] (within 0.2%). To obtain values for the product of molar density and binary diffusion coefficient of the ($\text{CH}_4 + \text{C}_2\text{H}_6$) system with the lowest possible uncertainty, we therefore recommend a scal-

ing of the calculated values by a factor of 0.995, which brings them into essentially perfect agreement with the values of Arora et al. [68]. For the ($\text{N}_2 + \text{C}_2\text{H}_6$) system, the recent data of McGovern and Manion [74] for the temperature range (300–723) K exhibit the best agreement with the calculated values with average absolute relative deviations of 1.2%. The strong disagreement of up to 8% between the calculated values and the MD-based correlation of Chae et al. [75] is probably primarily due to the use of the empirical OPLS force field [77] by Chae et al. Such a simple generic model cannot be expected to yield diffusion coefficients of the same order of accuracy as the system-specific, *ab initio*-based pair potentials of the present work.

Figures 11 and 12 also depict the results obtained with the unadjusted $\text{CH}_4\text{-C}_2\text{H}_6$ and $\text{N}_2\text{-C}_2\text{H}_6$ PESs for equimolar mixtures. The relative deviations from the values for the adjusted PESs at $T = 300$ K are $+1.12\%$ for the ($\text{CH}_4 + \text{C}_2\text{H}_6$) system and $+0.08\%$ for the ($\text{N}_2 + \text{C}_2\text{H}_6$) system. That the relative deviations are much larger compared with those for viscosity and thermal conductivity is due to the fact that, as already mentioned, the binary diffusion coefficient in the dilute gas phase depends essentially only on the unlike interactions.

Estimates of the relative combined expanded uncertainties ($k = 2$) of the calculated values for all three transport properties are given in the footnotes of Tables 2–4. If a scaling is recommended, the estimates refer to the scaled values. Note that these estimates are based mainly on experience. The largest source of

Table 4: Calculated values for the products of molar densities and binary diffusion coefficients, $\rho_m D$ (in $10^{-4} \text{ mol}\cdot\text{m}^{-1}\cdot\text{s}^{-1}$), of the mixtures ($\text{CH}_4 + \text{C}_2\text{H}_6$) and ($\text{N}_2 + \text{C}_2\text{H}_6$) in the dilute gas limit as a function of mole fraction x and temperature T .^a

T/K	CH_4 (1) + C_2H_6 (2)			N_2 (1) + C_2H_6 (2)		
	$x_1 \rightarrow 0$	$x_1 = 0.5$	$x_1 \rightarrow 1$	$x_1 \rightarrow 0$	$x_1 = 0.5$	$x_1 \rightarrow 1$
90	1.829	1.828	1.827	1.849	1.849	1.850
105	2.156	2.155	2.154	2.194	2.195	2.196
120	2.492	2.492	2.492	2.544	2.544	2.545
135	2.835	2.835	2.835	2.893	2.894	2.894
150	3.181	3.181	3.182	3.239	3.240	3.240
175	3.759	3.760	3.760	3.804	3.803	3.803
200	4.331	4.332	4.333	4.348	4.347	4.345
225	4.892	4.893	4.893	4.870	4.868	4.865
250	5.439	5.439	5.440	5.370	5.367	5.363
275	5.970	5.970	5.970	5.850	5.846	5.840
300	6.486	6.485	6.484	6.310	6.305	6.298
325	6.986	6.985	6.982	6.753	6.747	6.738
350	7.472	7.469	7.465	7.179	7.172	7.162
375	7.943	7.939	7.933	7.591	7.583	7.572
400	8.400	8.395	8.387	7.990	7.981	7.968
450	9.279	9.271	9.258	8.752	8.742	8.727
500	10.11	10.10	10.08	9.475	9.463	9.446
550	10.91	10.90	10.87	10.16	10.15	10.13
600	11.68	11.66	11.63	10.82	10.81	10.79
650	12.41	12.39	12.35	11.46	11.44	11.42
700	13.12	13.09	13.05	12.07	12.06	12.03
800	14.47	14.44	14.39	13.25	13.23	13.20
900	15.75	15.71	15.65	14.36	14.34	14.31
1000	16.98	16.93	16.85	15.43	15.41	15.38
1100	18.15	18.09	18.01	16.46	16.43	16.40
1200	19.28	19.22	19.12	17.45	17.42	17.39

^a The listed $\rho_m D$ values for the ($\text{CH}_4 + \text{C}_2\text{H}_6$) system should be scaled by a factor of 0.995 to obtain the recommended values. The relative combined expanded uncertainty ($k = 2$) of the scaled values is estimated to be 1.0% for temperatures from 250 K to 700 K and 2.0% otherwise. The respective estimate for the listed values of the ($\text{N}_2 + \text{C}_2\text{H}_6$) system is 2.0% from 250 K to 700 K and 3.0% otherwise.

uncertainty is probably the treatment of the molecules as rigid rotors. The use of the classical Hamilton equations instead of a quantum-mechanical approach to describe the rigid-rotor collision dynamics should be justified at any of the investigated temperatures, even at the lowest. We estimate that the neglect of third- and higher-order kinetic theory contributions to the thermal conductivity does not introduce errors of more than 0.2% at any temperature, whereas the errors resulting from the neglect of fourth- and higher-order contributions to the shear viscosity and the binary diffusion coefficient should be negligible. In addition to these systematic uncertainty contributions, the calculated transport property values have statistical uncertainties of the order of (0.1–0.2)% as already stated in Section 3.2.

5. Correlations

Practical correlations for the cross second virial coefficients of the two molecule pairs were obtained by fitting polynomials in $(T^*)^{-1/2}$ with $T^* = T/(100 \text{ K})$ to the semiclassical calculated values. We employed the symbolic regression software Eureka (version 1.24.0) [78] to find optimal polynomial structures. The resulting expression for the $\text{CH}_4\text{--C}_2\text{H}_6$ molecule

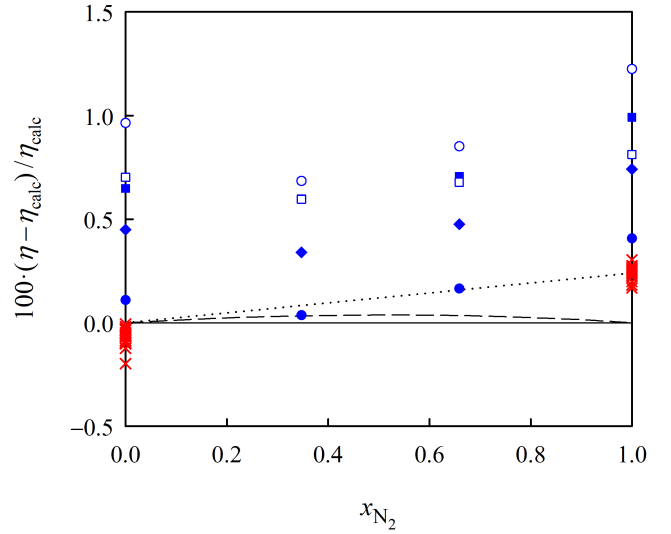


Figure 8: Relative deviations of experimental data for the dilute gas shear viscosity of the ($\text{N}_2 + \text{C}_2\text{H}_6$) system as a function of nitrogen mole fraction: ●, Abe et al. [55], 298 K; ○, Abe et al. [55], 333 K; ■, Abe et al. [55], 373 K; □, Abe et al. [55], 418 K; ◆, Abe et al. [55], 468 K; ×, Vogel [57] and Vogel et al. [58], (292–682) K for nitrogen and (291–624) K for ethane. The dashed and dotted lines indicate the values obtained with the unadjusted $\text{N}_2\text{--C}_2\text{H}_6$ PES at $T = 300 \text{ K}$ and the recommended values resulting from Eq. 10, respectively. For clarity of the figure, the stated uncertainties for the data of Abe et al. [55] (0.3%), Vogel [57] (0.2%) and Vogel et al. [58] (0.3%) are not indicated by error bars.

pair is

$$\frac{B_{12}^{\text{QFH}}}{\text{cm}^3\cdot\text{mol}^{-1}} = b_1 + \frac{b_2}{(T^*)^{1/2}} + \frac{b_3}{T^*} + \frac{b_4}{(T^*)^{5/2}} + \frac{b_5}{(T^*)^3} + \frac{b_6}{(T^*)^6}, \quad (11)$$

where $b_1 = 35.022$, $b_2 = 158.69$, $b_3 = -599.19$, $b_4 = -42.313$, $b_5 = -356.69$, and $b_6 = -75.742$. For $\text{N}_2\text{--C}_2\text{H}_6$, we obtained

$$\frac{B_{12}^{\text{QFH}}}{\text{cm}^3\cdot\text{mol}^{-1}} = b_1 + \frac{b_2}{(T^*)^{1/2}} + \frac{b_3}{T^*} + \frac{b_4}{(T^*)^3} + \frac{b_5}{(T^*)^6} + \frac{b_6}{(T^*)^8}, \quad (12)$$

where $b_1 = 34.160$, $b_2 = 141.14$, $b_3 = -458.57$, $b_4 = -181.50$, $b_5 = -15.381$, and $b_6 = -0.79500$. Equations (11) and (12) reproduce the calculated values within $\pm 0.012 \text{ cm}^3\cdot\text{mol}^{-1}$ and $\pm 0.014 \text{ cm}^3\cdot\text{mol}^{-1}$, respectively. Both correlations extrapolate reasonably to temperatures below 90 K and above 1200 K.

Correlations for $\rho_m D$ were developed in the same manner as in previous studies [12, 13, 61] using the calculated values of the present work. The values for the ($\text{CH}_4 + \text{C}_2\text{H}_6$) system were scaled by a factor of 0.995 as recommended in the previous section. For convenience, we neglected the small composition dependences of $\rho_m D$ and fitted the correlations to the values for equimolar mixtures. The basic form of the correlations is

$$\frac{10^4 \times \rho_m D}{\text{mol}\cdot\text{m}^{-1}\cdot\text{s}^{-1}} = \frac{\bar{T}^{1/2}}{S(\bar{T})}, \quad (13)$$

where $\bar{T} = T/\text{K}$. If $\rho_m D$ were to be obtained from the first-order kinetic theory, $S(\bar{T})$ would be proportional to a single

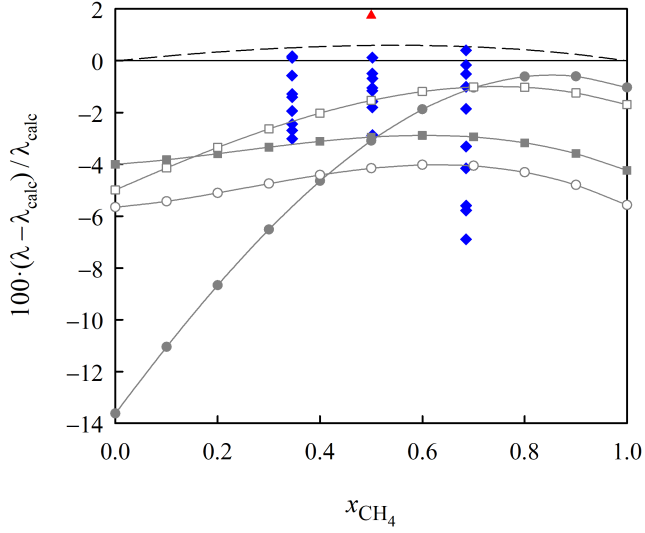


Figure 9: Relative deviations of experimental data and an experimentally based correlation for the dilute gas thermal conductivity of the $(\text{CH}_4 + \text{C}_2\text{H}_6)$ system from the calculated values of the present work as a function of methane mole fraction: \blacklozenge , Roder and Friend [62], (194–330) K; \blacktriangle , Sakonidou et al. [63], 311 K; \bullet , correlation by Friend and Roder [64] at 140 K; \circ , correlation by Friend and Roder [64] at 200 K; \blacksquare , correlation by Friend and Roder [64] at 270 K; \square , correlation by Friend and Roder [64] at 330 K. The dashed line indicates the values obtained with the unadjusted $\text{CH}_4\text{--C}_2\text{H}_6$ PES at $T = 300$ K. For clarity of the figure, the stated uncertainties for the data of Roder and Friend [62] (1.6%) are not indicated by error bars.

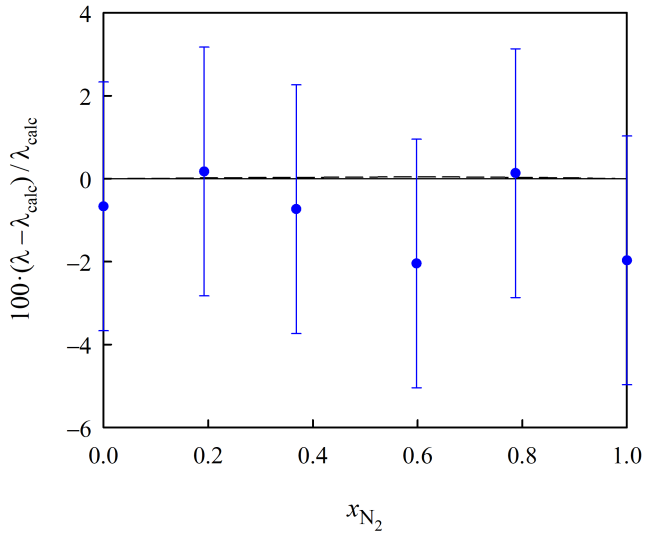


Figure 10: Relative deviations of experimental data for the dilute gas thermal conductivity of the $(\text{N}_2 + \text{C}_2\text{H}_6)$ system from the calculated values of the present work as a function of nitrogen mole fraction: \bullet , Gilmore and Comings [65], 348 K. The dashed line indicates the values obtained with the unadjusted $\text{N}_2\text{--C}_2\text{H}_6$ PES at $T = 300$ K.

generalized cross section, which decreases monotonically with temperature. To find functional forms for $S(\bar{T})$ that obey this

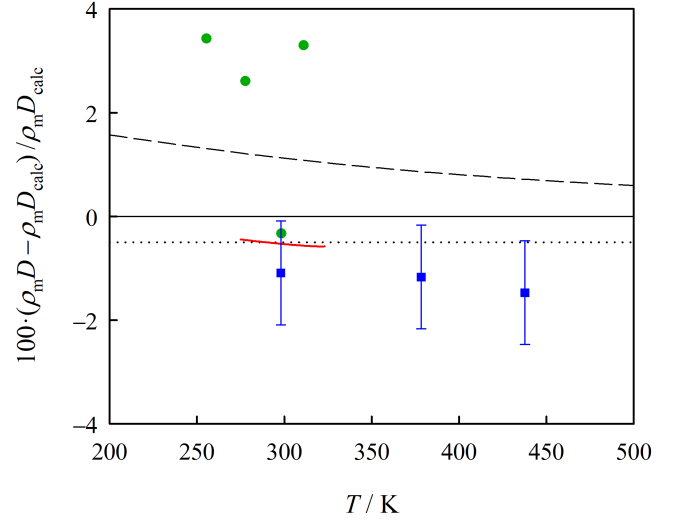


Figure 11: Relative deviations of experimental data for the product of molar density and binary diffusion coefficient of the $(\text{CH}_4 + \text{C}_2\text{H}_6)$ system in the dilute gas phase from the calculated values of the present work as a function of temperature: \bullet , Chang [66]; \blacksquare , Gotoh et al. [67]; solid line, Arora et al. [68] (provided by the authors only in the form of a smoothing function). The dashed and dotted lines indicate the values obtained with the unadjusted $\text{CH}_4\text{--C}_2\text{H}_6$ PES for an equimolar mixture and the recommended values resulting from scaling the calculated values by a factor of 0.995, respectively.

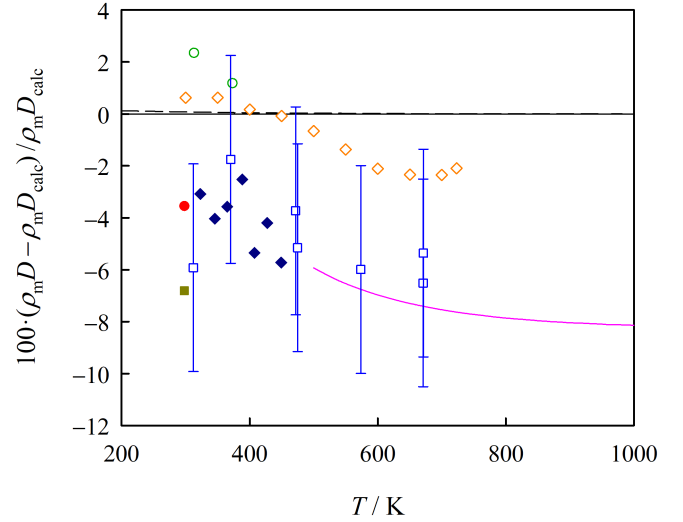


Figure 12: Relative deviations of experimental data for the product of molar density and binary diffusion coefficient of the $(\text{N}_2 + \text{C}_2\text{H}_6)$ system in the dilute gas phase from the calculated values of the present work as a function of temperature: \bullet , Boyd et al. [69]; \circ , Arai et al. [70]; \blacksquare , Jacobs et al. [71]; \square , Wakeham and Slater [72]; \blacklozenge , Katsanos and Karaiskakis [73]; \diamond , McGivern and Manion [74]. The solid line indicates the MD-based correlation by Chae et al. [75], while the dashed line indicates the values obtained with the unadjusted $\text{N}_2\text{--C}_2\text{H}_6$ PES.

constraint at any temperature (i.e., also at temperatures below 90 K and above 1200 K to ensure good extrapolation behavior),

while being both accurate and simple, the Eureka software was again used. Following the approach employed in our previous studies [12, 13, 61], \bar{T} was restricted to appear solely in integer powers of $\bar{T}^{1/6}$. Furthermore, only constants, exponential functions, and the operators addition, subtraction, multiplication, division, and negation were allowed. For the (CH₄ + C₂H₆) system, the following function found by Eureka fulfills all requirements:

$$S(\bar{T}) = d_1 + d_2 \exp(-\bar{T}^{1/6}) + d_3 \exp(-\bar{T}^{1/3}) + \bar{T}^{1/6} \exp(-2\bar{T}^{1/3}) \left[d_4 + d_5 \exp(-\bar{T}^{1/3}) \right], \quad (14)$$

where $d_1 = 1.2242$, $d_2 = 15.137$, $d_3 = 271.57$, $d_4 = -3842.3$, and $d_5 = 44604$. The correlation reproduces the scaled calculated $\rho_m D$ values within $\pm 0.02\%$. For the (N₂ + C₂H₆) system, only a less accurate three-parameter function, which reproduces the calculated values within $\pm 0.3\%$, was found to obey the requirement that $S(\bar{T})$ decreases monotonically with temperature:

$$S(\bar{T}) = d_1 + d_2 \exp(-\bar{T}^{1/6}) + d_3 \bar{T}^{1/6} \exp(-\bar{T}^{1/3}), \quad (15)$$

where $d_1 = 1.4738$, $d_2 = 13.363$, and $d_3 = 85.537$. For both systems, the correlations for $\rho_m D$ extrapolate in a physically reasonable manner to any temperature below 90 K or above 1200 K.

6. Conclusions

The cross second virial coefficients and dilute gas shear viscosities, thermal conductivities, and binary diffusion coefficients of the systems (CH₄ + C₂H₆) and (N₂ + C₂H₆) were determined with high accuracy at temperatures from 90 K to 1200 K using state-of-the-art computational approaches. The cross second virial coefficients were calculated by means of statistical thermodynamics, while the three transport properties were computed using the kinetic theory of molecular gases [7–11]. The required analytical PES models for CH₄–C₂H₆ and N₂–C₂H₆ interactions were developed as part of this study. They are based on supermolecular quantum-chemical *ab initio* calculations at the RI-MP2 [16, 17] and CCSD(T) [25] levels of theory for several thousand mutual configurations of the interacting molecules and are represented analytically by site-site potential functions. Both analytical PESs were fine-tuned to the best available experimental data for the cross second virial coefficients. Fortran 90 implementations of the PESs are provided in the [Supporting Information](#). The computation of the transport properties involves also the like-species interactions; the respective generalized cross sections were obtained in previous studies [2, 9] from our accurate analytical PESs for CH₄–CH₄ [1], N₂–N₂ [4], and C₂H₆–C₂H₆ [2] interactions.

The agreement between the calculated values for the investigated thermophysical properties of the two mixtures and the best available experimental data is overall very satisfactory and confirms the high accuracy of the calculated values. Moreover, the calculated values cover a much wider temperature range.

Thus, our knowledge of the thermophysical properties of these important mixtures is substantially improved.

Tables of the computed values for the investigated properties are provided together with estimates of their uncertainties. In the case of the shear viscosities of the two systems and the binary diffusion coefficient of the (CH₄ + C₂H₆) system, small empirical adjustments (which are within $\pm 0.5\%$) in the form of scaling factors are recommended. We also developed practical correlations for the cross second virial coefficients and the binary diffusion coefficients.

Even though the present results and those of our previous computational studies on nine further binary mixtures [9–14, 61] cover only the low-density gas phase, they provide an essential basis for the improvement of methods for estimating mixture properties also at higher densities by enforcing the correct low-density limiting behavior.

Funding

The author gratefully acknowledges financial support by the Deutsche Forschungsgemeinschaft (DFG) through Grant No. HE 6155/2-1.

Appendix A. Supplementary data

Supplementary data related to this article can be found at <https://doi.org/10.1016/j.jct.2019.03.002>.

References

- [1] R. Hellmann, E. Bich, E. Vogel, *Ab initio* intermolecular potential energy surface and second pressure virial coefficients of methane, *J. Chem. Phys.* 128 (21) (2008) 214303. doi:10.1063/1.2932103.
- [2] R. Hellmann, Reference Values for the Second Virial Coefficient and Three Dilute Gas Transport Properties of Ethane from a State-of-the-Art Intermolecular Potential Energy Surface, *J. Chem. Eng. Data* 63 (2) (2018) 470–481. doi:10.1021/acs.jced.7b01069.
- [3] R. Hellmann, Intermolecular potential energy surface and thermophysical properties of propane, *J. Chem. Phys.* 146 (11) (2017) 114304. doi:10.1063/1.4978412.
- [4] R. Hellmann, *Ab initio* potential energy surface for the nitrogen molecule pair and thermophysical properties of nitrogen gas, *Mol. Phys.* 111 (3) (2013) 387–401. doi:10.1080/00268976.2012.726379.
- [5] R. Hellmann, *Ab initio* potential energy surface for the carbon dioxide molecule pair and thermophysical properties of dilute carbon dioxide gas, *Chem. Phys. Lett.* 613 (2014) 133–138. doi:10.1016/j.cplett.2014.08.057.
- [6] R. Hellmann, E. Bich, E. Vogel, V. Vesovic, *Ab initio* intermolecular potential energy surface and thermophysical properties of hydrogen sulfide, *Phys. Chem. Chem. Phys.* 13 (30) (2011) 13749–13758. doi:10.1039/C1CP20873J.
- [7] F. R. W. McCourt, J. J. M. Beenakker, W. E. Köhler, I. Kušćer, *Nonequilibrium Phenomena in Polyatomic Gases, Vol. I: Dilute Gases*, Clarendon Press, Oxford, 1990.
- [8] A. S. Dickinson, R. Hellmann, E. Bich, E. Vogel, Transport properties of asymmetric-top molecules, *Phys. Chem. Chem. Phys.* 9 (22) (2007) 2836–2843. doi:10.1039/B618549E.
- [9] R. Hellmann, E. Bich, E. Vogel, V. Vesovic, Intermolecular potential energy surface and thermophysical properties of the CH₄–N₂ system, *J. Chem. Phys.* 141 (22) (2014) 224301. doi:10.1063/1.4902807.
- [10] R. Hellmann, E. Bich, V. Vesovic, Calculation of the thermal conductivity of low-density CH₄–N₂ gas mixtures using an improved kinetic theory approach, *J. Chem. Phys.* 144 (13) (2016) 134301. doi:10.1063/1.4945014.

- [11] R. Hellmann, E. Bich, V. Vesovic, Cross second virial coefficients and dilute gas transport properties of the (CH₄ + CO₂), (CH₄ + H₂S), and (H₂S + CO₂) systems from accurate intermolecular potential energy surfaces, *J. Chem. Thermodyn.* 102 (2016) 429–441. doi:10.1016/j.jct.2016.07.034.
- [12] J.-P. Crusius, R. Hellmann, J. C. Castro-Palacio, V. Vesovic, *Ab initio* intermolecular potential energy surface for the CO₂–N₂ system and related thermophysical properties, *J. Chem. Phys.* 148 (21) (2018) 214306. doi:10.1063/1.5034347.
- [13] R. Hellmann, Thermophysical Properties of Gaseous H₂S–N₂ Mixtures from First-Principles Calculations, *Z. Phys. Chem.*, published online. doi:10.1515/zpch-2018-1250.
- [14] R. Hellmann, Cross Second Virial Coefficients and Dilute Gas Transport Properties of the (CH₄ + C₃H₈) and (CO₂ + C₃H₈) Systems from Accurate Intermolecular Potential Energy Surfaces, *J. Chem. Eng. Data* 63 (1) (2018) 246–257. doi:10.1021/acs.jced.7b00886.
- [15] S. F. Boys, F. Bernardi, The calculation of small molecular interactions by the differences of separate total energies. Some procedures with reduced errors, *Mol. Phys.* 19 (4) (1970) 553–566. doi:10.1080/00268977000101561.
- [16] F. Weigend, M. Häser, RI-MP2: first derivatives and global consistency, *Theor. Chem. Acc.* 97 (1-4) (1997) 331–340. doi:10.1007/s002140050269.
- [17] F. Weigend, M. Häser, H. Patzelt, R. Ahlrichs, RI-MP2: optimized auxiliary basis sets and demonstration of efficiency, *Chem. Phys. Lett.* 294 (1-3) (1998) 143–152. doi:10.1016/S0009-2614(98)00862-8.
- [18] F. Weigend, M. Kattannek, R. Ahlrichs, Approximated electron repulsion integrals: Cholesky decomposition versus resolution of the identity methods, *J. Chem. Phys.* 130 (16) (2009) 164106. doi:10.1063/1.3116103.
- [19] S. Kossmann, F. Neese, Comparison of two efficient approximate Hartree-Fock approaches, *Chem. Phys. Lett.* 481 (4-6) (2009) 240–243. doi:10.1016/j.cpllett.2009.09.073.
- [20] T. H. Dunning, Jr., Gaussian basis sets for use in correlated molecular calculations. I. The atoms boron through neon and hydrogen, *J. Chem. Phys.* 90 (2) (1989) 1007–1023. doi:10.1063/1.456153.
- [21] R. A. Kendall, T. H. Dunning, Jr., R. J. Harrison, Electron affinities of the first-row atoms revisited. Systematic basis sets and wave functions, *J. Chem. Phys.* 96 (9) (1992) 6796–6806. doi:10.1063/1.462569.
- [22] F. Weigend, A fully direct RI-HF algorithm: Implementation, optimised auxiliary basis sets, demonstration of accuracy and efficiency, *Phys. Chem. Chem. Phys.* 4 (18) (2002) 4285–4291. doi:10.1039/B204199P.
- [23] F. Weigend, A. Köhn, C. Hättig, Efficient use of the correlation consistent basis sets in resolution of the identity MP2 calculations, *J. Chem. Phys.* 116 (8) (2002) 3175–3183. doi:10.1063/1.1445115.
- [24] A. Halkier, T. Helgaker, P. Jørgensen, W. Klopper, H. Koch, J. Olsen, A. K. Wilson, Basis-set convergence in correlated calculations on Ne, N₂, and H₂O, *Chem. Phys. Lett.* 286 (3-4) (1998) 243–252. doi:10.1016/S0009-2614(98)00111-0.
- [25] K. Raghavachari, G. W. Trucks, J. A. Pople, M. Head-Gordon, A fifth-order perturbation comparison of electron correlation theories, *Chem. Phys. Lett.* 157 (6) (1989) 479–483. doi:10.1016/S0009-2614(89)87395-6.
- [26] F. Neese, The ORCA program system, *WIREs Comput. Mol. Sci.* 2 (1) (2012) 73–78. doi:10.1002/wcms.81.
- [27] CFOUR, Coupled-Cluster techniques for Computational Chemistry, a quantum-chemical program package by J. F. Stanton, J. Gauss, M. E. Harding, P. G. Szalay with contributions from A. A. Auer, R. J. Bartlett, U. Benedikt, C. Berger, D. E. Bernholdt, Y. J. Bomble, L. Cheng, O. Christiansen, M. Heckert, O. Heun, C. Huber, T.-C. Jagau, D. Jonsson, J. Jusélius, K. Klein, W. J. Lauderdale, D. A. Matthews, T. Metzroth, L. A. Mück, D. P. O’Neill, D. R. Price, E. Prochnow, C. Puzzarini, K. Ruud, F. Schiffmann, W. Schwalbach, S. Stopkowitz, A. Tajti, J. Vázquez, F. Wang, J. D. Watts and the integral packages MOLECULE (J. Almlöf and P. R. Taylor), PROPS (P. R. Taylor), ABACUS (T. Helgaker, H. J. Aa. Jensen, P. Jørgensen, and J. Olsen), and ECP routines by A. V. Mitin and C. van Wüllen. For the current version, see <http://www.cfour.de>.
- [28] K. T. Tang, J. P. Toennies, An improved simple model for the van der Waals potential based on universal damping functions for the dispersion coefficients, *J. Chem. Phys.* 80 (8) (1984) 3726–3741. doi:10.1063/1.447150.
- [29] S. M. Cybulski, T. P. Haley, New approximations for calculating dispersion coefficients, *J. Chem. Phys.* 121 (16) (2004) 7711–7716. doi:10.1063/1.1795652.
- [30] R. P. Feynman, A. R. Hibbs, *Quantum Mechanics and Path Integrals*, McGraw-Hill, New York, 1965.
- [31] J. K. Singh, D. A. Kofke, Mayer Sampling: Calculation of Cluster Integrals using Free-Energy Perturbation Methods, *Phys. Rev. Lett.* 92 (22) (2004) 220601. doi:10.1103/PhysRevLett.92.220601.
- [32] B. Jäger, R. Hellmann, E. Bich, E. Vogel, *Ab initio* virial equation of state for argon using a new nonadditive three-body potential, *J. Chem. Phys.* 135 (8) (2011) 084308. doi:10.1063/1.3627151.
- [33] L. Waldmann, Transporterscheinungen in Gasen von mittlerem Druck, in: S. Flügge (Ed.), *Handbuch der Physik*, Vol. 12, Springer-Verlag, Berlin, 1958, pp. 295–514. doi:10.1007/978-3-642-45892-7_4.
- [34] L. Waldmann, E. Trübenbacher, Formale kinetische Theorie von Gasgemischen aus anregbaren Molekülen, *Z. Naturforsch. A* 17 (5) (1962) 363–376. doi:10.1515/zna-1962-0501.
- [35] J. H. Ferziger, H. G. Kaper, *The Mathematical Theory of Transport Processes in Gases*, North-Holland, Amsterdam, 1972.
- [36] C. F. Curtiss, Classical, diatomic molecule, kinetic theory cross sections, *J. Chem. Phys.* 75 (3) (1981) 1341–1346. doi:10.1063/1.442140.
- [37] M. Mustafa, Measurement and Calculation of Transport Properties of Polyatomic Gases, Ph.D. thesis, Imperial College London, London, UK (1987). doi:10044/1/47198.
- [38] E. L. Heck, A. S. Dickinson, Transport and relaxation cross-sections for pure gases of linear molecules, *Comput. Phys. Commun.* 95 (2-3) (1996) 190–220. doi:10.1016/0010-4655(96)00033-1.
- [39] U. Setzmann, W. Wagner, A New Equation of State and Tables of Thermodynamic Properties for Methane Covering the Range from the Melting Line to 625 K at Pressures up to 100 MPa, *J. Phys. Chem. Ref. Data* 20 (6) (1991) 1061–1155. doi:10.1063/1.555898.
- [40] R. Span, E. W. Lemmon, R. T. Jacobsen, W. Wagner, A. Yokozeki, A reference Equation of State for the Thermodynamic Properties of Nitrogen for Temperatures from 63.151 to 1000 K and Pressures to 2200 MPa, *J. Phys. Chem. Ref. Data* 29 (6) (2000) 1361–1433. doi:10.1063/1.1349047.
- [41] D. Bücker, W. Wagner, A Reference Equation of State for the Thermodynamic Properties of Ethane for Temperatures from the Melting Line to 675 K and Pressures up to 900 MPa, *J. Phys. Chem. Ref. Data* 35 (1) (2006) 205–266. doi:10.1063/1.1859286.
- [42] E. L. Heck, A. S. Dickinson, Transport and relaxation properties of N₂, *Mol. Phys.* 81 (6) (1994) 1325–1352. doi:10.1080/00268979400100911.
- [43] E. M. Dantzler, C. M. Knobler, M. L. Windsor, Interaction virial coefficients in hydrocarbon mixtures, *J. Phys. Chem.* 72 (2) (1968) 676–684. doi:10.1021/j100848a049.
- [44] C. J. Wormald, E. J. Lewis, D. J. Hutchings, Excess enthalpies of gaseous mixtures of *n*-alkanes, *J. Chem. Thermodyn.* 11 (1) (1979) 1–12. doi:10.1016/0021-9614(79)90076-4.
- [45] T. Katayama, K. Ohgaki, H. Ohmori, Measurement of interaction second virial coefficients with high accuracy, *J. Chem. Eng. Jpn.* 13 (4) (1980) 257–262. doi:10.1252/jcej.13.257.
- [46] M. Jaeschke, S. Audibert, P. van Caneghem, A. E. Humphreys, R. Janssen-van Rosmalen, Q. Pellei, J. P. J. Michels, J. A. Schouten, C. A. ten Seldam, GERG Tech. Monogr. TM2, Verlag des Vereins Deutscher Ingenieure, Düsseldorf, 1988.
- [47] P. J. McElroy, J. Fang, Compression factors and virial coefficients of (methane + ethane), *J. Chem. Thermodyn.* 26 (6) (1994) 617–623. doi:10.1006/jcht.1994.1071.
- [48] J. P. M. Trusler, The speed of sound in (0.8CH₄ + 0.2C₂H₆)(g) at temperatures between 200 K and 375 K and amount-of-substance densities up to 5 mol·dm⁻³, *J. Chem. Thermodyn.* 26 (7) (1994) 751–763. doi:10.1006/jcht.1994.1089.
- [49] W. Blanke, R. Weiss, Virial coefficients of methane-ethane mixtures in the temperature range from 0 to 60°C determined with an automated expansion apparatus, *Int. J. Thermophys.* 16 (3) (1995) 643–653. doi:10.1007/BF01438849.
- [50] H. Hou, J. C. Holste, K. R. Hall, K. N. Marsh, B. E. Gammon, Second and Third Virial Coefficients for Methane + Ethane and Methane + Ethane + Carbon Dioxide at (300 and 320) K, *J. Chem. Eng. Data* 41 (2) (1996) 344–353. doi:10.1021/je9502307.

- [51] J. H. Dymond, K. N. Marsh, R. C. Wilhoit, in: M. Frenkel, K. N. Marsh (Eds.), *Landolt-Börnstein: Numerical Data and Functional Relationships in Science and Technology: New Series, Vol. 21B: Virial Coefficients of Mixtures of Group IV: Physical Chemistry*, Springer, Berlin-Heidelberg-New York, 2002, Ch. 3, p. 283. doi:10.1007/b98915.
- [52] H. J. Achtermann, G. Magnus, H. M. Hinze, M. Jaeschke, *PVT data from refractive index measurements for the ethane + nitrogen system from 270 to 350 K and pressures to 28 MPa*, *Fluid Phase Equilib.* 64 (1991) 263–280. doi:10.1016/0378-3812(91)90018-3.
- [53] E. S. Lopatinskii, M. S. Rozhnov, V. I. Zhdanov, S. L. Parnovskii, Y. N. Kudrya, *Second virial coefficient of gas mixtures of hydrocarbons, carbon dioxide and hydrogen with nitrogen and argon*, *Zh. Fiz. Khim.* 65 (1991) 2060–2065.
- [54] Y. Abe, J. Kestin, H. E. Khalifa, W. A. Wakeham, *The viscosity and diffusion coefficients of the mixtures of four light hydrocarbon gases*, *Physica A* 93 (1-2) (1978) 155–170. doi:10.1016/0378-4371(78)90215-7.
- [55] Y. Abe, J. Kestin, H. E. Khalifa, W. A. Wakeham, *The Viscosity and Diffusion Coefficients of the Mixtures of Light Hydrocarbons with Other Polyatomic Gases*, *Ber. Bunsenges. Phys. Chem.* 83 (3) (1979) 271–276. doi:10.1002/bbpc.19790830315.
- [56] E. Vogel, *Reference Viscosities of Gaseous Methane and Hydrogen Sulfide at Low Density in the Temperature Range from (292 to 682) K*, *J. Chem. Eng. Data* 56 (7) (2011) 3265–3272. doi:10.1021/jc200371n.
- [57] E. Vogel, *Towards Reference Viscosities of Carbon Monoxide and Nitrogen at Low Density Using Measurements between 290 K and 680 K as well as Theoretically Calculated Viscosities*, *Int. J. Thermophys.* 33 (5) (2012) 741–757. doi:10.1007/s10765-012-1185-1.
- [58] E. Vogel, R. Span, S. Herrmann, *Reference Correlation for the Viscosity of Ethane*, *J. Phys. Chem. Ref. Data* 44 (4) (2015) 043101. doi:10.1063/1.4930838.
- [59] E. Vogel, C. Küchenmeister, E. Bich, A. Laesecke, *Reference Correlation of the Viscosity of Propane*, *J. Phys. Chem. Ref. Data* 27 (5) (1998) 947–970. doi:10.1063/1.556025.
- [60] E. Vogel, *The Viscosities of Dilute Kr, Xe, and CO₂ Revisited: New Experimental Reference Data at Temperatures from 295 K to 690 K*, *Int. J. Thermophys.* 37 (2016) 63. doi:10.1007/s10765-016-2068-7.
- [61] R. Hellmann, *Cross second virial coefficient and dilute gas transport properties of the (H₂O + CO₂) system from first-principles calculations*, *Fluid Phase Equilib.* 485 (2019) 251–263. doi:10.1016/j.fluid.2018.11.033.
- [62] H. M. Roder, D. G. Friend, *Thermal Conductivity of Methane-Ethane Mixtures at Temperatures Between 140 and 330 K and at Pressures up to 70 MPa*, *Int. J. Thermophys.* 6 (6) (1985) 607–617. doi:10.1007/BF00500333.
- [63] E. P. Sakonidou, H. R. van den Berg, C. A. ten Seldam, J. V. Sengers, *The thermal conductivity of an equimolar methane-ethane mixture in the critical region*, *J. Chem. Phys.* 109 (2) (1998) 717–736. doi:10.1063/1.476611.
- [64] D. G. Friend, H. M. Roder, *The Thermal Conductivity Surface for Mixtures of Methane and Ethane*, *Int. J. Thermophys.* 8 (1) (1987) 13–26. doi:10.1007/BF00503221.
- [65] T. F. Gilmore, E. W. Comings, *Thermal conductivity of binary mixtures of carbon dioxide, nitrogen, and ethane at high pressures: Comparison with correlation and theory*, *AIChE J.* 12 (6) (1966) 1172–1178. doi:10.1002/aic.690120623.
- [66] G. T. Chang, *Diffusion in dilute and moderately dense gases by a perturbation technique*, Ph.D. thesis, Rice University, Houston, Texas (1966).
- [67] S. Gotoh, M. Manner, J. P. Sørensen, W. E. Stewart, *Binary Diffusion Coefficients of Low-Density Gases. I. Measurements by Modified Loschmidt Method*, *J. Chem. Eng. Data* 19 (2) (1974) 169–171. doi:10.1021/jc60061a025.
- [68] P. S. Arora, H. L. Robjohns, T. N. Bell, P. J. Dunlop, *Use of binary diffusion and second virial coefficients to predict viscosities of gaseous systems*, *Aust. J. Chem.* 33 (9) (1980) 1993–1996. doi:10.1071/CH9801993.
- [69] C. A. Boyd, N. Stein, V. Steingrimsson, W. F. Rumpel, *An Interferometric Method of Determining Diffusion Coefficients in Gaseous Systems*, *J. Chem. Phys.* 19 (5) (1951) 548–553. doi:10.1063/1.1748290.
- [70] K. Arai, S. Saito, S. Maeda, *On the Dispersion Mechanism in Laminar Flow through Tubes*, *Kagaku Kogaku* 31 (1967) 25–31. doi:10.1252/kakoronbunshu1953.31.25.
- [71] T. Jacobs, L. Peeters, J. Vermant, *Binary Diffusion Coefficients of Lower Alkanes in Nitrogen and Argon*, *Bull. Soc. Chim. Belges* 79 (5-6) (1970) 337–341. doi:10.1002/bscb.19700790509.
- [72] W. A. Wakeham, D. H. Slater, *Diffusion coefficients for n-alkanes in binary gaseous mixtures with nitrogen*, *J. Phys. B* 6 (5) (1973) 886–896. doi:10.1088/0022-3700/6/5/024.
- [73] N. A. Katsanos, G. Karaiskakis, *Temperature variation of gas diffusion coefficients measured by the reversed-flow sampling technique*, *J. Chromatog. A* 254 (1983) 15–25. doi:10.1016/S0021-9673(01)88314-X.
- [74] W. S. McGivern, J. A. Manion, *Hydrocarbon binary diffusion coefficient measurements for use in combustion modeling*, *Combust. Flame* 159 (10) (2012) 3021–3026. doi:10.1016/j.combustflame.2012.04.015.
- [75] K. Chae, P. Elvati, A. Violi, *Effect of Molecular Configuration on Binary Diffusion Coefficients of Linear Alkanes*, *J. Phys. Chem. B* 115 (3) (2011) 500–506. doi:10.1021/jp109042q.
- [76] B. Jäger, E. Bich, *Thermophysical properties of krypton-helium gas mixtures from *ab initio* pair potentials*, *J. Chem. Phys.* 146 (21) (2017) 214302. doi:10.1063/1.4984100.
- [77] W. L. Jorgensen, D. S. Maxwell, J. Tirado-Rives, *Development and Testing of the OPLS All-Atom Force Field on Conformational Energetics and Properties of Organic Liquids*, *J. Am. Chem. Soc.* 118 (45) (1996) 11225–11236. doi:10.1021/ja9621760.
- [78] M. Schmidt, H. Lipson, *Distilling Free-Form Natural Laws from Experimental Data*, *Science* 324 (5923) (2009) 81–85. doi:10.1126/science.1165893.